Environmental Science Nano

Effect of protein corona on nanoparticle-plasma membrane and nanoparticle-biomimetic membrane interactions

Journal:	*Environmental Science: Nano*
Manuscript ID	EN-ART-01-2020-000035
Article Type:	Paper

Environmental Significance Statement for:

Effect of protein corona on nanoparticle-plasma membrane and nanoparticle-biomimetic membrane interactions

Ubiquitous nanoscale environmental pollutant particles represent a serious hazard to public health. The toxicity of nanoparticles can be affected by formation of protein coronas around these particles in biological environments. The effect of the protein corona needs to be assessed not only *in vitro*, but also with simplified models to find the mechanism underlying how the corona modulates nanomaterial-biomembrane interactions. Our study using cell lines, isolated cell membranes, and biomimetic membranes made from natural lipid extract demonstrates the protective role of the protein corona in non-specific nanomaterial-biomembrane interactions. This comparison between plasma membranes and biomimetic membranes establishes the limits of model membranes as tool in predicting the potential health risks of nanoparticles.

Effect of protein corona on nanoparticle-plasma membrane and nanoparticle-biomimetic membrane interactions

Lu Wang,[a] Nicolas Hartel,[a] Kaixuan Ren,[a] Nicholas Alexander Graham,[a] Noah Malmstadt*[abc]

[a] *Mork Family Department of Chemical Engineering and Materials Science, 925 Bloom Walk, University of Southern California, Los Angeles, California 90089-1211, United States.*
E-mail: malmstad@usc.edu
[b] *Department of Chemistry, 840 Downey Way, University of Southern California, Los Angeles, California 90089-0744, United States*
[c] *Department of Biomedical Engineering, 3650 McClintock Avenue, University of Southern California, Los Angeles, California 90089-1111, United States*

Abstract

Nanomaterial contamination in the environment poses severe threats to public health and wellness. Understanding interactions between nanoparticles and biomembranes is pivotal to understanding the physiological effects of nanomaterials. The prevailing understanding is that a protein corona forms around nanoparticles upon their entering biological systems. The effect of the protein corona on the membrane-nanoparticle interaction has not been comprehensively investigated. Here, we report a systematic study to better understand the effects of the protein corona on nanoparticle-biomembrane interactions with both plasma membranes (293T cell line) and biomimetic membranes. Giant plasma membrane vesicles (GPMVs) and giant unilamellar vesicles (GUVs) fabricated from organ lipid extracts (brain, heart, and liver) served as biomimetic models in our study. Reduced charged-nanoparticle adhesion to both plasma and biomimetic membranes with the presence of the protein corona suggests that the protein corona interferes with the electrostatic interaction between nanoparticles and biomembranes. These similar trends of nanoparticle adhesion among the membranes indicated that model membranes can capture this electrostatic interaction with similar responses as plasma membranes. However, the membrane integrity subsequent to the interaction was different between the two systems, indicating the limitations of model membranes in recreating the complexity and dynamics of plasma membranes. As the first systematic study correlating nanoparticle interactions with cell membranes, isolated cell membranes, and synthetic vesicles from natural lipid extracts, we demonstrated that biomimetic membranes can serve as excellent analogues to cell membranes in providing fundamental insights regarding the electrostatic interaction between nanoparticles and biomembranes.

Introduction

Nanomaterial contamination in the environment is present in forms such as ultrafine soot and nanoplastics. Ultrafine soot with adverse respiratory health effects is heavily emitted from diesel and gasoline exhaust. The hazardous accumulation of nanoplastics in aquatic and terrestrial environment originates not only from production and usage lifecycle degradation of extensively used plastics, but also from the fragmentation in landfills. Engineered nanomaterials, with applications in biosensors, bioimaging and drug delivery, are also becoming increasingly deployed. Given the increasing presence of nanomaterials in day-to-day experience, the potential hazards posed to biological systems by nanoparticles have become a notable concern. The interplay between nanoparticles and cells can lead to cellular accumulation of nanoparticles, compromised

plasma membrane integrity, as well as mitochondrial and lysosomal damage.[1, 2] These potentially cytotoxic effects are determined by nanoparticle characteristics such as size, shape, charge, and surface chemistry.[3]

Nanoparticles adsorb proteins and other biomolecules upon entering biological fluids due to their high surface energy. The associated proteins, called the protein corona, modify the surface properties of the nanoparticles, providing them with biological properties distinct from those they would have in their pristine state, thereby altering the fate of nanoparticles in biological systems.[4, 5] There remain many open questions regarding the role of the protein corona.[6] It has been generally believed that the protein corona protects cells against reactive surfaces of nanoparticles and increases the safety of nanomedicines.[7, 8] But Obst and her colleagues found that the protein corona does not significantly decrease cellular uptake of nanoparticles into macrophages.[9] In some cases, the protein corona can even activate surface receptors and lead to undesired immune responses.[10, 11] It is well known that the initial step in cellular uptake of nanoparticles is dominated by interfacial interactions between the plasma membrane and nanoparticles, and the cytotoxicity of nanoparticles has been related to this interaction.[12, 13] Therefore, a systematic knowledge of the nanoparticle-plasma membrane interaction is the key to understanding this nano-bio interfacial phenomena and the impact of the protein corona on cells.

To date, the interpretation of nanoparticle-membrane behaviors in *in vitro* experiments is still not well established due to the complex and dynamic nature of cell membranes. Simplified biological model membranes are advantageous to perform focused studies and systematic investigations of the nanoparticle-biomembrane interface.[14] Giant unilamellar vesicles (GUVs) and giant plasma membrane vesicles (GPMVs) are representative free-standing model biomembranes: they are bottom-up and top-down approaches for mimicking plasma membranes, respectively. GUVs are fabricated from tunable lipid ingredients and can be designed to present representative lipid compositions in plasma membranes.[15, 16] GPMVs are blebs isolated from cells that have a composition similar or identical to that of the plasma membrane; they largely preserve the plasma membrane's physical properties while being free from contamination of organelle membranes.[17, 18] These simple and stable model membranes have shown clear similarities with *in vitro* studies in terms of non-specific interactions with nanoparticles,[19] particularly not only validating pathways of nanoparticle internalization but also strongly correlating membrane distortion with cell viability.[20, 21] Our previous studies utilizing GUVs have further unveiled the an adhesion-based mechanism contributing to toxicity of charged nanoparticles.[22, 23]

It is important to correlate cellular process with biophysical phenomena to identify general mechanisms underlying the cellular process.[24] Here we report a comprehensive attempt to investigate the impact of the protein corona on non-specific interactions between charged nanoparticles and plasma membranes by establishing a correlation between plasma membranes and biomimetic membranes. We selected representative nanoplastic polystyrene nanoparticles (PNPs) for our study. In addition to examining charged PNP interactions with cell surfaces, we used GUVs fabricated from natural lipid extracts and GPMVs from 293T cells. We observed interactions between the membranes and PNPs with and without a protein corona, and further compared PNP adsorption to membranes as well as membrane integrity upon PNP interaction. Through this study, we have confirmed the general protective effect of protein corona in non-specific electrostatic nanoparticle-biomembrane interactions. This systematic study also suggests that model membranes are reliable platforms to explore the nano-bio interface, providing fundamental information for nanomaterial design in clinical and environmental applications.

Materials and methods

Materials. Green fluorescent 100 nm diameter polystyrene nanoparticles were purchased from Magsphere, CA. 1,2-dioleoyl-sn-glycero-3-phosphocholine (DOPC), 1-palmitoyl-2-oleoyl-glycero-3-phosphocholine (POPC), cholesterol as well as brain, heart, and liver total lipid extract were purchased from Avanti Polar Lipid, AL. 1,1′-dioctadecyl-3,3,3′,3′- tetramethylindodicarbocyanine, 4-chlorobenzenesulfonate salt (DiD) and CF633 labeled wheat germ agglutinin (CF633-WGA) were purchased from Biotium, CA. Phosphate buffered saline (PBS), Dulbecco's phosphate-buffered saline with calcium and magnesium (DPBS), penicillin/streptomycin, L-glutamine, and trypsin were obtained from Corning, NY. Dulbecco's modified Eagle's medium (DMEM) and fetal bovine serum (FBS) were purchased from Gibco, MA. DAPI stain, 10 kDa rhodamine-dextran, BCA assay kit and LDH assay kit were purchased from ThermoFisher Scientific, MA. Human male type AB serum (H4522) was purchased from Sigma Aldrich, MO. 293T cell line was obtained from the American Type Culture Collection (ATCC), VA. Other reagents were purchased from Sigma Aldrich, MO.

Protein corona preparation and quantification. 5 mg/mL PNPs (15 nM) were incubated in human male type AB serum (Sigma Aldrich, MO) for 30 min at 37 °C under gentle shaking. Unbound proteins were separated from PNP–protein complexes with centrifugation (16,100 g, 20 min). Pellets were then washed three times with PBS buffer and then resuspended in PBS buffer; PNPs with protein corona (PNP/corona) were hereby obtained. Unbound proteins in the supernatant were quantified by a bicinchonicic acid (BCA) assay for each wash. Using a PNP-absent control sample with the same starting concentration of human serum, the amount of proteins extracted by PNPs can be calculated through the BCA assay results.

Protein corona elution and SDS-PAGE. Proteins were eluted from PNP/corona particles by adding elution buffer (95% 2X Laemmili buffer, 5% beta-mercaptoethanol, BioRad) and heating at 95 °C for 5 min. Then eluted proteins were separated by centrifuging out the PNPs (16,100 g, 25 min). Proteins harvested from 0.1 mg (0.3 pmol) PNPs were analyzed by SDS-PAGE using precast 4%-20% Mini-PROTEAN TGX polyacrylamide gels (BioRad). Color prestained protein standard (11-245 kDa) (BioLabs) was used as a molecular weight marker and the gels were run for 30 min at 200 V in Tris-Glycine-SDS buffer. Gels were then stained using Coomassie Blue Protein stain.

Proteomic analysis. To avoid noise introduced by surfactant in the LC-MS system, Laemmili buffer cannot be used for protein elution, so here we used a paramagnetic bead isolation method separate from the one for SDS-PAGE.[25] Protein corona was eluted from 0.5 mg (1.5 pmol) PNPs by adding 500 µL 8M urea buffer, heating at 95 °C for 20 min. Proteins were then reduced by incubating with 5 mM dithiothreitol (DTT) at 45 °C for 30 min. Alkylation was induced by incubating with 25 mM iodoacetamide (IAA) at room temperature for 30 min in dark followed by quenching with 10 mM DTT. 30 µL each of Sera-Mag Beads A (Thermo CAT No. 09-981-121) and Sera Mag Beads B (Thermo CAT No. 09-981-123) were combined and washed with 200 µL of water 3 times. 500 µg of beads were added to each 500 µL protein sample. 500 µL of ethanol was added and samples were incubated for 8 min at room temperature. Supernatant was then removed. 200 µL 70% ethanol was added and incubated for 30 min twice, and the supernatant was removed each time. 180 µL of ethanol was added and the supernatant removed. Samples were reconstituted in 100 µL of digestion buffer (50 mM HEPES, pH 8, 10 µg trypsin) and incubated overnight at 37 °C. The samples were sonicated to improve peptide recovery. The supernatant was collected and dried in a SpeedVac. Samples were resuspended in 100 µL of 0.1% Trifluoroacetic acid (TFA) and desalted on C18 STAGE tips, and eluted with 30% Acetonitrile, 0.1% TFA. Eluates were dried, resuspended in 10 µL of 0.1% Formic Acid and injected onto an EasynLC1200 which was directly

electrosprayed into a Q-Exactive Plus Mass Spectrometer. RAW data was processed on Proteome Discoverer 2.2 with human FASTA file downloaded from *UniProt*.

DLS and zeta potential measurement. DLS and zeta potential measurements were taken on a Wyatt Mobius mobility instrument. Samples of PNPs in PBS were prepared at a concentration of 0.5 mg/mL (1.5 nM). Samples of PNPs in cell culture media were prepared by adding PNPs (1 mg/mL in PBS, 3 nM) to the culture media at a concentration of 0.1 mg/mL (0.3 nM), the samples were equilibrated for 5 min before the measurements. Measurements were taken at 25 °C with 5 s run time. Diameters and zeta potentials are reported as averages and standard deviations of ten and three acquirements, respectively.

Cell culture and imaging. 293T cells were cultured in complete cell culture medium (cMEM), consisting of DMEM supplemented with 10% FBS along with 1% penicillin/streptomycin and 2 mM L-glutamine. Cells were grown in a 5% CO_2 incubator at 37 °C, passaged using trypsin. Cells were treated with PNPs by replacing culture medium with DMEM containing 0.1 mg/mL PNPs (0.3 nM). For imaging, cells were fixed with 4% paraformaldehyde, and stained with 1 μg/mL DAPI and 5 μg/mL CF633-WGA, then observed with a spinning disk confocal microscope (Nikon Eclipse TiE equipped with a Yokogawa confocal head). Quantification of PNP adhesion was achieved by measuring the intensity of green fluorescence colocalized with the cells, and this intensity was calibrated versus a control group where PNPs were absent to eliminate background fluorescence. Mean fluorescence was normalized based on the cell area.

Cell viability MTT assay. 293T cells were cultured in 96-well plates overnight with a seeding density of 1×10^5 cell/mL in 0.1 mL cDMEM, followed by incubation with 0.1 mg/mL PNPs (0.3 nM) in DMEM or cMEM at 37 °C for 4 h and 15 h. Untreated cells were used as a negative control. The incubation media was then replaced with 3-(4,5-dimethylthiazol-2-yl)-2,5-diphenyltetrazolium bromide (MTT) (Sigma Aldrich, MO) dissolved in cMEM (0.5 mg/mL) to start the assay. Formazan was allowed to form during 4 h incubation at 37 °C. The formed formazan was dissolved in DMSO and absorbance at 550 nm was measured with a microplate reader (Synergy H1; BioTek). Each sample was analyzed in four replicates. No interference of the PNPs present in solution with MTT was found in the absorbance measurement.

Lactate dehydrogenase (LDH) release assay. 293T cells were cultured in 96-well plates overnight with a seeding density of 1×10^5 cell/mL in 0.1 mL cDMEM, and then treated with 0.1 mg/mL PNPs (0.3 nM) in DMEM or cMEM, incubating at 37 °C for 4 h and 15 h. LDH assays were carried out according to the manufacturer's instruction. The percentage of released LDH was normalized by the amount of LDH from complete lysis of control cells. Four replicates were used for each condition. And no noticeable assay activity between PNPs and LDH assay buffer was found.

GPMV preparation. At 70%-80% cell confluence, GPMVs were isolated by chemical induced cell blebbing with 25 mM paraformaldehyde and 2 mM dithiothreitol in DPBS buffer for 1 h at 37 °C. The membrane dye DiD was added to the GPMV suspension at a concentration of 5 μg/mL.

GUV preparation. The GUVs were prepared by the agarose rehydration method.[26] The agarose hydration method was selected as it avoids oxidative degradation of lipids as in the alternative electro-formation method, and it is more capable of incorporating charged lipids thus preserving most of the natural lipid compositions.[27] Despite the possible existence of agarose residue encapsulated in the GUVs,[28] our study focuses on the interplay on the surface of the membranes, agarose hydration method is preferred in our study. Our previous work with agarose hydration shows that vesicles made via this method maintain

expected liquid-liquid phase segregation behavior, suggesting that any agarose present introduces minimal biophysical artifacts.[29, 30] Brain, heart and liver total lipid extract were dissolved in chloroform; heart total lipid extract requires addition of 10 wt% cholesterol to form GUVs. The lipid solution was deposited on 2 wt% agarose-coated coverslips. After chloroform evaporation, PBS buffer was added to rehydrate the lipid film. The membrane dye DiD was incorporated in the rehydration buffer with a final concentration of 5 μg/mL. The lipid film was rehydrated at 37 °C for 30 min and GUVs were harvested afterwards.

Microscopy imaging of model vesicles and quantification. Microscopy images were taken with a spinning disk confocal microscope (Nikon Eclipse TiE equipped with a Yokogawa confocal head). PNPs and calcein can be captured with 491 nm laser excitation, 10 kDa rhodamine dextran can be captured with 561 nm laser excitation and DiD dye with 640 nm. To avoid crosstalk between different dyes, emission signals were collected independently in serial mode. Images were acquired at constant laser power and exposure time. Model membrane samples were held in glass-bottom multiwell plates treated with bovine serum albumin (BSA) and rinsed three times with PBS. Images were taken at the equatorial plane of each vesicle.

For PNP adhesion observation, the GPMV or GUV suspension was loaded into BSA-treated wells and then incubated with 0.1 mg/mL (0.3 nM) PNPs. PNP adhesion was observed and recorded after incubation at room temperature for 4 h and 15 h. Control groups left out PNPs, but same volume of PBS buffer was added instead. Quantification of PNP adhesion was achieved by measuring the intensity of green fluorescence colocalized with the membranes (the outer contour and inner contour of each vesicle were identified, and the intensity of nanoparticle fluorescence was measured only between these two contours). The fluorescence was then normalized based on the circumference of the membrane at the equatorial plane to allow for comparison between vesicles with different sizes. This normalized fluorescence intensity was further calibrated by subtracting the normalized intensity from the control group to eliminate background fluorescence.

For the membrane integrity study, the GPMV or GUV suspension was loaded into BSA-treated wells with 1mg/mL calcein in PBS buffer (or 1mg/mL 10 kDa rhodamine-dextran in PBS buffer) at a 1:1 ratio, followed by PNP addition to a final concentration of 0.1 mg/mL (0.3 nM). The osmolarity of calcein buffer or dextran buffer was balanced with the vesicle suspensions. Control groups were identical with the exception of PNP addition; the same volume of PBS buffer was added instead. Quantification was carried out by calculating the fractional population of vesicles with calcein leaked into the lumen. We set the threshold to be ten percent of the background fluorescence intensity, vesicles whose fluorescence intensity differences across membranes were less than this threshold were categorized as leaked vesicles.

Results and Discussion

Protein corona characterization

Electrostatics can play fundamental roles in nanoparticle-biomembrane interactions and in the fate of nanoparticles in biological systems.[1, 22, 23] Polystyrene nanoparticles (PNPs) at 100 nm diameter with surface functionalization of negatively charged sulfate groups (sulfate-PNPs), negatively charged carboxyl groups (carboxyl-PNPs), and positively charged amine groups (amine-PNPs) were selected in this study. PNPs were all labeled with an encapsulated green fluorophore (491 nm excitation, 509 nm emission). After treatment with human serum at 37 °C for 30 min with gentle shaking, protein coronas were formed on these three types of PNPs. The protein corona composition with this prolonged incubation time should be more equilibrated compared to the rapid corona formation at early exposure.[8] The hydrodynamic diameters of PNPs after treatment with human serum increased (Table 1 and Figure S1), indicating the existence of

proteins bound to the surfaces of the PNPs. Sulfate-PNPs and positively charge amine-PNPs with protein corona displayed upward shifts (~20 nm) in mean sizes. Negatively charged carboxyl-PNPs had a broadened size distribution and the largest increase of mean size. This might be attributed to aggregation of the particles, but since the size distribution was below 600 nm, the aggregation clusters might only consist of a few particles. Zeta potential measurement showed the expected negative surface charges for the sulfate-PNPs and carboxyl-PNPs, as well as positive surface charge of the amine-PNPs. After incubation with human serum, the surface zeta potential for all three of PNPs became close to the value for human serum. Proteins from human serum not only covered the surface of PNPs, but also altered charge properties of the PNPs.

Table 1. Properties of the polystyrene nanoparticles with and without protein corona. All measurements were performed in PBS buffer; protein mass was determined via BCA assay.

	Hydrodynamic diameter ± s.d. (nm)		Zeta potential ± s.d. (mV)		mg protein/ mg PNPs
	No corona	With corona	No corona	With corona	
SPNP*	94.27 ± 2.66	118.50 ± 10.4	-45.22 ± 4.89	-9.56 ± 3.00	0.212
CPNP*	87.53 ± 2.8	198.21 ± 71.68	-37.99 ± 4.42	-10.16 ± 2.82	0.575
APNP*	101.44 ± 14.94	122.29 ± 11.66	20.31 ± 3.29	-9.50 ± 3.48	0.096

*SPNP: 100 nm sulfate-functionalized polystyrene nanoparticles; CPNP: 100 nm carboxyl-functionalized polystyrene nanoparticles; APNP: 100 nm amine-functionalized polystyrene nanoparticles.

The characterization of the protein corona was achieved by elution, quantification, separation, and identification. Among the three types of PNPs, carboxyl-PNPs were eluted with the most abundant proteins, which echoed the change in carboxyl-PNP size distribution with protein corona: the broadened distribution and relatively extreme size increase might be caused by large amounts of protein bound to carboxyl-PNPs. According to SDS-PAGE (Figure 1a), eluted protein coronas from all types of particles shared a strong band at around 25 kDa, and major differences were observed in the range of 50-100 kDa and below 17 kDa.

For a better understanding of protein identities in the coronas, proteomic analysis of eluted protein coronas was carried out with LC-MS-MS. Proteins identified with at least two peptides are listed in Table S1. We found out that proteins existed in coronas of all three types of PNPs were mainly apolipoproteins with molecular weights corresponding to the bands around 25 kDa on SDS-PAGE. Apolipoproteins have been discovered previously as a major group of proteins in the corona formed around nanoparticles of different materials upon contact with plasma.[31, 32] Apolipoproteins are involved in the transportation of lipids and cholesterol in the bloodstream, thereby they could greatly affect the intracellular trafficking and fate of nanoparticles in biological environments.[33] Highly abundant human serum albumin (HSA) was not substantially found in the gel analysis or in the proteomic study, this might be due to it being replaced by the higher-affinity and slower-exchanging apolipoproteins.[34] While the abundant proteins were observed in the coronas of all types of PNPs and there were many proteins shared between PNPs (Figure 1b), protein corona composition varied slightly depending on the surface charge of the PNPs. Through classifying the proteins by their isoelectric point (pI), negatively charged carboxyl-PNP and sulfate-PNP coronas were enriched with proteins with pI higher than 6, and positively charged amine-PNP coronas were enriched with proteins with pI values lower than 6 (Figure 1c). This difference in pI values can be explained by the attraction between oppositely charged species.[8] In conclusion, these three types of PNPs formed protein coronas with different quantities and diverse identities of proteins, while they shared the dominant proteins as observed in SDS-PAGE results. They showed different preferences in protein charge due to electrostatic attraction such that all corona-coated particles bore similar surface charges.

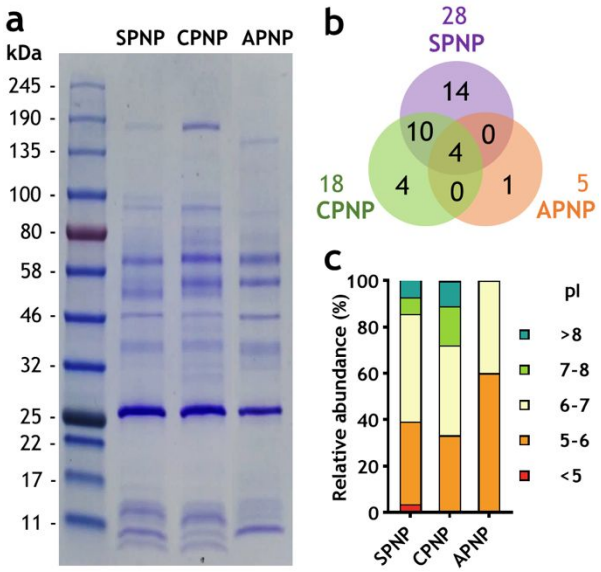

Figure 1. Comparison of protein corona composition on sulfate-, carboxyl-, and amine-polystyrene nanoparticles (SPNPs, CPNPs, and APNPs respectively). (a) Coomassie blue-stained SDS-PAGE gel of human plasma proteins obtained from corona on SPNPs, CPNPs, and APNPs. (b) LC-MS-MS result of proteins identified in the corona formed on SPNPs, CPNPs, and APNPs. This Venn diagram reports the number of unique proteins identified from each of three nanoparticles as well as proteins common to two or all three nanoparticle populations. (c) Classification of corona proteins identified by LC-MS-MS according to their calculated isoelectric point (pI); relative percentages are shown.

Cell-PNP interactions

We have studied the perturbation of cell membranes induced by PNPs. After incubation with PNPs for 4 h in protein-free culture media, 293T cells were fixed and fluorescently stained. The fluorescence images of nuclei (DAPI, blue channel), cell membranes (CF633-WGA, red channel) and PNPs (green channel) were merged in Figure 2a. In the condition where protein corona was absent, the sulfate-PNPs showed almost no colocalization with cells, carboxyl- and amine PNPs were adsorbed onto cell membranes. The adhesion of carboxyl-PNPs onto cell membranes might suggest binding of negatively charged carboxyl-PNPs with the rare positively charged domains on cell membranes.[35, 36] Moreover, the positively charged moiety of the zwitterionic lipid headgroups can attract negatively charged carboxyl-PNPs.[37] While regarding positively charged amine-PNPs, not only strong binding to cell membranes was observed, but cellular damage was also discovered with shrinkage of the cell volume and loss of nuclear boundaries. All these adhesions and damages were alleviated with the presence of a protein corona. A similar trend was observed after 15 h incubation. In general, there was no notable increase in fluorescence intensity from 4 h (Figure S2), indicating the PNP adhesion had reached equilibrium before or around 4 h.

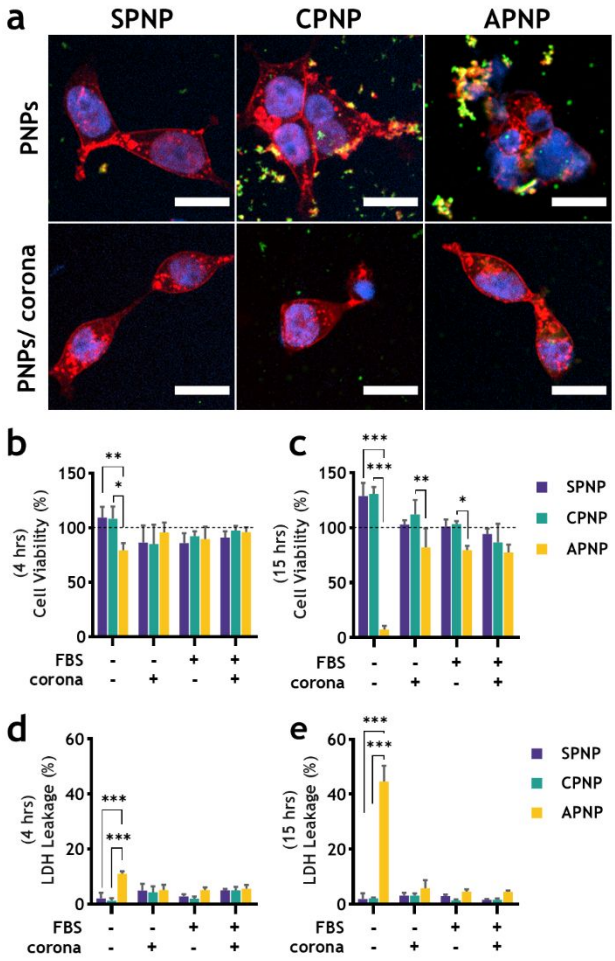

Figure 2. Effect of the protein corona on cellular adhesion of nanoparticles and cell viability. Sulfate-PNPs, carboxyl-PNPs, and amine-PNPs are denoted as SPNP, CPNP, and APNP. (a) Confocal microscopy images of 293T cells show that adsorption of nanoparticles was reduced with the presence of a protein corona. Images were taken after 4 h incubation of the cells with nanoparticles in FBS-free culture media. The green channel corresponds to the fluorescently labeled nanoparticles, blue channel corresponds to DAPI stained nuclei, and red fluorescence signal comes from CF633-WGA stained cell membranes. The scale bars are 30 μm. (b, c) Cell viability of 293T cells exposed to nanoparticles. Cells were incubated with nanoparticles for (b) 4 h and (c) 15 h, under conditions of presence or absence of protein corona as well as FBS included or excluded from the culture medium. Cell viability was evaluated using the MTT assay, the viability is normalized based on the control group where no PNPs were added. LDH leakage of 293T cells exposed to nanoparticles for (d) 4 h and (e) 15 h were assessed, under conditions of presence or absence of protein corona as well as FBS included or excluded from the culture medium, the leakage percentage is normalized based on the negative control group (0%) where no PNPs were added and the positive control group (100%) where cells were treated with lysis buffer. (Unpaired t-test, * significant at $p < .05$, ** significant at $p < .01$, *** significant at $p < .001$, detailed test results are listed in Table S3 and Table S4)

Aside from the morphological changes of the cells and estimation of PNP adhesion, the acute toxicity of the PNPs with and without protein corona was assessed by MTT and LDH assays. The MTT assay evaluates the mitochondrial activity which is related to cell viability, and the LDH assay evaluates the release of the cytoplasmic enzyme LDH as a consequence of membranes leaking in damaged or dead cells.[38, 39] Since the presence of fetal bovine serum (FBS) in cell culture media might contribute to formation of a protein corona

on the PNPs, assays were carried out also with conditions where FBS was omitted.[40] We assessed cell viability and membrane integrity over 4 h and 15 h. At the 4 h time point (Figure 2b), cell viability decreased to 80% with native amine-PNPs, but in the presence of FBS or protein corona the damage from these positively charge amine-PNPs was mitigated, which is in accordance with the microscopy images in Figure 2a. The viability at the 15 h time point was more drastically affected by amine-PNPs: direct contact between amine-PNPs and cells induced around 90% viability loss, cell viability was decreased to 80% even with FBS or protein corona reducing the damage (Figure 2c). As for LDH assays (Figure 2d and 2e), 293T cells had the most significant cytoplasm leakage with positively charged amine-PNPs, for both 4 h and 15 h time points. Again, the presence of proteins in the cell culture medium and proteins on the surface of PNPs both alleviated the damage to membrane integrity. This can be explained by the high surface energy of nanoparticles. Nanoparticles tend to form coronas if not from proteins and other biomolecules in the medium, then from cellular components. Therefore, without proteins in the media, PNPs with their pristine surface would likely rupture the cell membranes and extract biomolecules to reduce their surface energy. Once the PNP surface was pre-treated with protein and surface energy reduced by the protein corona, the damage to the cell membranes was alleviated.[7] In addition to the surface energy, electrostatic interactions with negatively charged cell membranes can play an important role as well.[41] Zeta potential has been measured for all three types of PNPs in all the conditions tested in the viability or leakage assay (Table S2). Both FBS in culture media and protein corona treatment maintained negative charges on initially negatively charged PNPs, while the native amine-PNPs in FBS-absent culture media presented slight aggregation and unstable surface charges including both negative and positive charges. The zeta potential result was in line with the cell viability and leakage data, as positive charge is prone to be more cytotoxic. The adhesion of PNPs was established and stabilized within the first 4 hours, while the cytotoxicity in MTT assay and LDH assay were majorly developed from 4 h to 15 h. This suggests that the cytotoxic effects are the result of events that occur subsequent to PNP-membrane interactions.

Biomimetic membrane-PNP interaction

Since lipid bilayers are the fundamental architectural structures in cell membranes, the non-specific interactions and adhesions of nanoparticles with minimal models of lipid bilayers can be correlated to the nanoparticle interactions with cell membranes. Four types of biomimetic membrane vesicles--GPMVs harvested from 293T cell line, GUVs fabricated from brain, heart, and liver lipid extract were incubated with PNPs for 4 h and 15 h. The results among all four model membranes were similar (Figure 3a, Figure S3), and it was worth noting that no penetration of PNPs through membranes was observed. There was a clear colocalization of fluorescence signal between positively charged amine-PNPs and model membranes, while the negatively charged sulfate-PNPs and carboxyl-PNPs showed some aggregation and occasional adhesion to the membranes. Yet all the adhesion was strongly diminished in the presence of protein corona. The amount of PNP adhesion was evaluated through quantification of the green fluorescence overlaying with the membranes (Figure 3b), the fluorescence intensity was normalized by circumference of the membranes at the equatorial plane facilitating comparison between vesicles of different sizes. The fluorescent intensity of bound amine-PNPs with protein corona (amine-PNP/corona) was significantly lower than that of amine-PNPs without corona. Meanwhile, sulfate-PNPs and carboxyl-PNPs showed low fluorescent intensity regardless of corona formation. This universal trend among four model membranes was in line with the toxicity of amine-PNPs and strong electrostatic binding of amine-PNPs to 293T cells, as well as the effect of the protein corona revealed with 293T cells in the previous section.

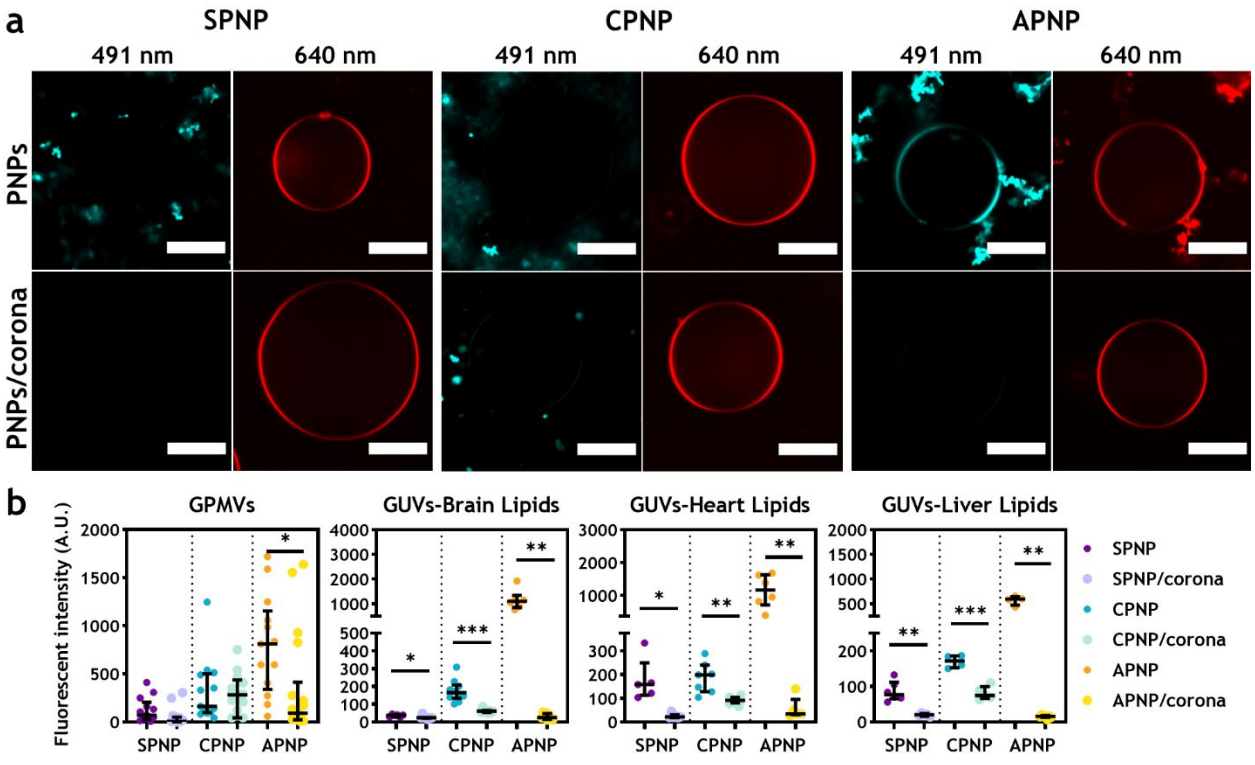

Figure 3. Effect of the protein corona on nanoparticle binding to biomimetic membranes. Sulfate-PNPs, carboxyl-PNPs, and amine-PNPs are denoted as SPNP, CPNP and APNP. (a) Confocal microscopy image of DiD-stained brain lipid GUVs (640 nm excitation) and green fluorescent nanoparticles (491 nm excitation) after 4 h incubation. (scale bar: 30 μm). (b) Fluorescent intensity of adsorbed nanoparticles on lipid membranes of GPMVs and GUVs after 4 h incubation. Medians and interquartile ranges of calibrated fluorescence intensity were demonstrated along with individual values in graphs. The adsorption of amine-PNPs (APNPs) was significantly decreased by protein corona (Unpaired t-test, * significant at $p < .05$, ** significant at $p < .01$, *** significant at $p < .001$)

Interestingly, negatively charged sulfate-PNPs and carboxyl-PNPs were found to adhere less aggressively to model membranes compared to cell membranes, while the adhesion of positively charged amine-PNPs appeared to be more aggressive. This can be explained by the lipid composition of model membranes. The formation of GPMVs is accompanied by a significant enrichment of negatively charged phosphatidylserine (PS) lipids to the outer membrane leaflet and degradation of negatively charged phosphatidylinositol (PI) lipids, making it unlikely for GPMVs to bear positive charges.[42] As for the lipid extracts composing GUVs, the lipid headgroups are mostly negatively charged according to the manufacturer. We believed that electrostatic interaction is an essential part of the nanomaterial-biomembrane interaction. In this regard, model membranes can essentially capture nanoparticle interaction as expected in cells, especially when electrostatic interactions dominate. However, model membranes cannot fully reflect plasma membranes, as they do not necessarily recreate the asymmetry of charge on plasma membranes. This effect can be investigated by fabricating asymmetric vesicles via microfluidic technique or fabricating vesicles from purely inner leaflet or outer leaflet lipid compositions.[43, 44]

The development of PNP adhesion on model membranes was further studied after 15 h incubation; the results from 15 h incubation showed similar behaviors, where amine-PNP binding significantly decreased in the presence of a protein corona (Figure S4). Similar to plasma membranes, there was no apparent

increase of PNP fluorescence between the two time points in model membranes, suggesting that the quantity of PNPs on membranes had reached equilibrium before 4 h incubation.

Leakage of biomimetic membranes with PNPs

As a comparison to the LDH assay of the 293T cells, the leakage of the model membranes was also studied. Calcein release assays are well-established tools for assessing membrane damage.[45, 46] The poly-anionic nature of calcein molecule makes it membrane impermeable under normal physiological conditions, therefore the flux of calcein across membranes indicates compromised membrane integrity. To achieve comparable experimental conditions with LDH assays of 293T cells, we incubated the GPMVs and GUVs with PNPs for the same time scales in calcein buffer, and we observed the influx of calcein from the surrounding medium into the lumen. Sample images of model membrane vesicles in the presence of positively charged amine-PNPs and amine-PNP/corona are shown in Figure 4a. Although both PNPs and calcein appear in the green fluorescence channel, the fluorescence intensity inside the vesicles can be considered solely coming from calcein inflow, as PNPs were found not penetrating across model membranes in previous experiments. There was large vesicle-to-vesicle variation of leakage behavior within each sample. The vesicle-to-vesicle heterogeneity of GUVs may be caused by demixing of lipids in the dry film before rehydration.[47] And GPMVs can have varied compositions depending on local surface density of cells they derive from.[48] Therefore, integrity of model membranes with complex lipid compositions should be investigated based on population.

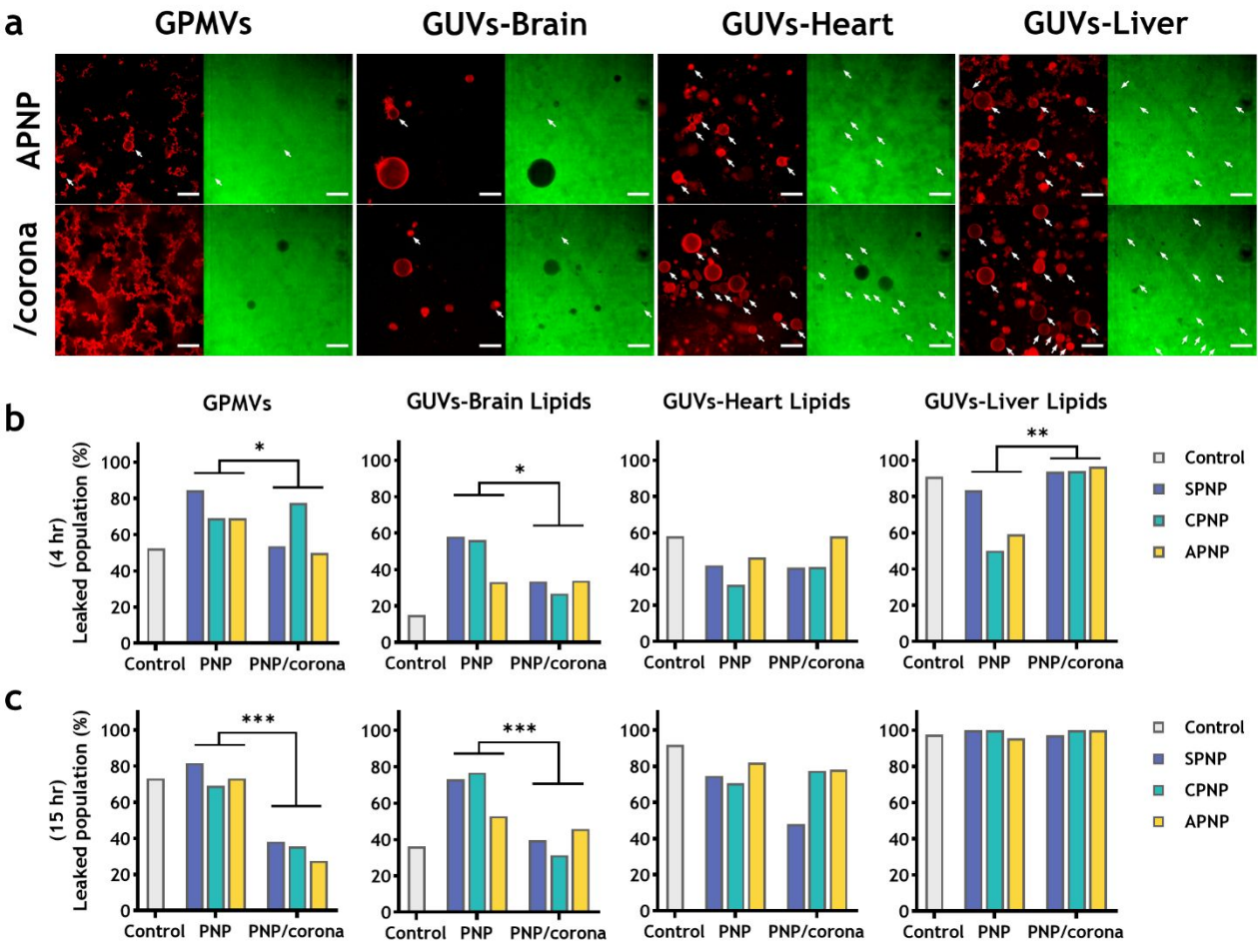

Figure 4. Effect of PNPs and protein corona on model membrane integrity. Sulfate-PNPs, carboxyl-PNPs, and amine-PNPs are denoted as SPNP, CPNP and APNP. (a) Confocal microscopy image of DiD-stained model membrane vesicles (red fluorescence) in 0.5 mg/mL calcein (green fluorescence) buffer after 15 h exposure to nanoparticles. White arrows point at the vesicles that had calcein leakage through membranes (scale bars in GUV panels: 60 μm; scale bars in GPMV panels: 30 μm). (b-c) Population of leaked vesicles after treatment of PNPs. Percentages of leaked vesicles after 4 h (b) and 15 h (c) incubation with PNPs are presented in graphs companied with control groups where PNPs were absent. (Unpaired t-test, * significant at $p < .05$, ** significant at $p < .01$, *** significant at $p < .001$)

Figures 4b and 4c compare the fraction of vesicle population that leaked under various conditions. The control groups of GPMVs, heart lipid GUVs, and liver lipid GUVs have notable high population of leakage even when no PNPs were added. One might relate this with the diffusivity of the membranes, as previous studies suggest that calcein can be facilitated by membrane characteristics such as high membrane fluidity and low packing density.[49] Liver lipid extract might have the highest fluidity due to the presence unsaturated lipids or short lipid tails, since it has the lowest phase transition temperature among the three lipid extracts.[50] Based on this premise, we conducted a control leakage assay with GUVs fabricated from pure DOPC, which possess phase transition temperature as low as -2 °C, and relative high diffusivity among the common phospholipids.[51] The DOPC GUVs did not show leakage unless nanoparticles were added (Figure S5), the leakage of control group maintained 0% even after 15 h. This is in line with our previous study showing membrane pore formation happens when nanoparticles adhere and impose surface tension onto the membrane surface.[22] While this result suggests against the hypothesis that high diffusivity leads to leakage in control groups, there have been studies demonstrating that oxidized lipid in the lipid bilayers can lead to pore formation, where these transient pores can have sizes above 545 Å.[52, 53] We speculate that lipid oxidation might have occurred during lipid extraction and GPMV isolation. Due to control group leakage in other model membranes, only brain lipid GUVs can be used to assess the effect of protein coronas in the calcein leakage assay. The differences in the three types of PNPs were not as obvious as the differences in membrane adhesion, so we grouped the three types of the PNPs to evaluate the effect of the protein corona. The group in the absence of protein corona had more leaked population. This result is in line with the aforementioned mechanism: protein coronas minimize PNP adhesion, and subsequent pore formation is hence reduced.

To investigate this mechanism further, we performed the calcein leakage assays with GUVs fabricated from pure DOPC lipid and pure POPC lipid (Figure S5). The trend observed here was similar to that observed for brain lipid GUVs. This common result between complex lipid extract and single lipid GUVs suggest that the pore formation on model membranes is not dependent on the surface charge of the PNPs and strong adhesion as observed for positively charged PNPs might not be required for pore formation, while the hydrophobic particle surface may be the dominant factor.[54] Therefore, the protein corona can reduce leakage by minimizing the possible contact of the hydrophobic surface to biomembranes.

We also conducted a leakage assay using 10 kDa rhodamine-dextran (Figure S6). The control groups of brain lipid GUVs and heart lipid GUVs showed lower leakage population with increasing leakage molecular size, indicating their pore sizes might be smaller than other model membranes. Similar to the calcein leakage assays mentioned previously, there are significant differences between the groups without and with coronas, however, the differences between membrane types were more obvious. Taken together, leakage assay results suggest that the pore formation is not dependent on the charge of the PNPs, that the presence of a

protein corona can alleviate pore formation, but the major factor affecting membrane integrity in contact with the PNPs lies in the intrinsic properties of the model membranes.

The LDH leakage of 293T cells occurred a relatively lower extent, and significant leakage from positively charged amine-PNPs can be distinguished from control group and groups without strong PNP adhesion. This suggests that cellular plasma membranes were more stable in the presence of nanoparticles, and that membrane integrity disruption might be due to a different mechanism. Plasma membranes are supported and tethered by the cytoskeleton, and the lateral diffusivity of lipid molecules in plasma membrane can be one order of magnitude lower than it in free-standing GUVs.[55, 56] The cytoskeleton not only restrains the diffusion of lipid molecules, but it can also work as a physical diffusion barrier in the influx and efflux transport of charged molecules and macromolecules.[19, 57] We can conclude that biomimetic membranes cannot fully recreate transport phenomena (particularly leakage) across cell membranes, as in terms of passive transport, lateral diffusivities of lipid molecules are different in the two systems. Furthermore, the cellular uptake and removal of charged or large molecules is mostly regulated by active transport. While at the same time, the simplified compositions make model membranes excellent for studying nano-bio interfacial phenomena on the lipid level without interference from other factors.

Conclusion

We have studied the effect of the protein corona on nanoparticle-biomembrane interactions. Through investigating these non-specific nanoparticle-biomembrane interactions by establishing a correlation between plasma membranes and biomimetic membranes, we have made the following conclusions: Protein corona composition depends on the surface charge of nanoparticles, but in general, it reduces nanoparticle adhesion and damage to the biomembranes. This is possibly due to surface energy stabilization and charge modification that comes with the corona. As a crucial part of this interplay, electrostatic interaction between nanoparticles and plasma membranes can be correlated with cytotoxicity of the nanoparticles. It is advantageous that model membranes such as GPMVs and GUVs can relate with plasma membranes through this fundamental interaction with similar responses. However, the model membranes have their limitations as their simplified composition does not mimic the complexity and dynamics in plasma membranes, such as differences in fluidity and tethering from cytoskeleton.

This study recognized the toxicity of positively charged nanoparticles and the general protective effect of the protein corona in the interplay between nanomaterials and biomembranes, providing insights about the relationship between electrostatic interactions and biological system perturbation caused by nanoparticles. Furthermore, defining the limits of the correlation between plasma membranes and biomimetic membranes has revealed promising applications of model membranes in studying nano-biomembrane interface interactions. It also provides an approach for studying these phenomena by reducing them into simplified models that isolate individual biophysical aspects of the system.

Conflicts of interest

There are no conflicts of interest to declare.

Acknowledgement

This article is based on work supported by the Office of Naval Research under N00014-16-1-2382. We gratefully acknowledge William E. Evenson for help in performing SDS-PAGE analysis. The 293T cell line was generously provided by Dr. Pin Wang's group. DLS and zeta potential measurement was carried

out with advisement from Dr. Shuxing Li in NanoBiophysics facility center at the Dornsife College of Letters, Arts, and Sciences at USC.

References

1. E. Fröhlich, The role of surface charge in cellular uptake and cytotoxicity of medical nanoparticles, *International journal of nanomedicine*, 2012, **7**, 5577.
2. N. Lewinski, V. Colvin and R. Drezek, Cytotoxicity of nanoparticles, *small*, 2008, **4**, 26-49.
3. S. Behzadi, V. Serpooshan, W. Tao, M. A. Hamaly, M. Y. Alkawareek, E. C. Dreaden, D. Brown, A. M. Alkilany, O. C. Farokhzad and M. Mahmoudi, Cellular uptake of nanoparticles: journey inside the cell, *Chem. Soc. Rev.*, 2017, **46**, 4218-4244.
4. M. Mahmoudi, I. Lynch, M. R. Ejtehadi, M. P. Monopoli, F. B. Bombelli and S. Laurent, Protein− nanoparticle interactions: opportunities and challenges, *Chem. Rev.*, 2011, **111**, 5610-5637.
5. M. P. Monopoli, C. Åberg, A. Salvati and K. A. Dawson, Biomolecular coronas provide the biological identity of nanosized materials, *Nature nanotechnology*, 2012, **7**, 779.
6. C. Corbo, R. Molinaro, A. Parodi, N. E. Toledano Furman, F. Salvatore and E. Tasciotti, The impact of nanoparticle protein corona on cytotoxicity, immunotoxicity and target drug delivery, *Nanomedicine*, 2016, **11**, 81-100.
7. A. Lesniak, F. Fenaroli, M. P. Monopoli, C. Åberg, K. A. Dawson and A. Salvati, Effects of the presence or absence of a protein corona on silica nanoparticle uptake and impact on cells, *ACS nano*, 2012, **6**, 5845-5857.
8. S. Tenzer, D. Docter, J. Kuharev, A. Musyanovych, V. Fetz, R. Hecht, F. Schlenk, D. Fischer, K. Kiouptsi and C. Reinhardt, Rapid formation of plasma protein corona critically affects nanoparticle pathophysiology, *Nature nanotechnology*, 2013, **8**, 772.
9. K. Obst, G. Yealland, B. Balzus, E. Miceli, M. Dimde, C. Weise, M. Eravci, R. Bodmeier, R. Haag and M. Calderón, Protein corona formation on colloidal polymeric nanoparticles and polymeric nanogels: impact on cellular uptake, toxicity, immunogenicity, and drug release properties, *Biomacromolecules*, 2017, **18**, 1762-1771.
10. Z. J. Deng, M. Liang, M. Monteiro, I. Toth and R. F. Minchin, Nanoparticle-induced unfolding of fibrinogen promotes Mac-1 receptor activation and inflammation, *Nature nanotechnology*, 2011, **6**, 39.
11. Y. Yan, K. T. Gause, M. M. Kamphuis, C.-S. Ang, N. M. O'Brien-Simpson, J. C. Lenzo, E. C. Reynolds, E. C. Nice and F. Caruso, Differential roles of the protein corona in the cellular uptake of nanoporous polymer particles by monocyte and macrophage cell lines, *ACS nano*, 2013, **7**, 10960-10970.
12. C. M. Sayes, J. D. Fortner, W. Guo, D. Lyon, A. M. Boyd, K. D. Ausman, Y. J. Tao, B. Sitharaman, L. J. Wilson and J. B. Hughes, The differential cytotoxicity of water-soluble fullerenes, *Nano Lett.*, 2004, **4**, 1881-1887.
13. P. J. Smith, M. Giroud, H. L. Wiggins, F. Gower, J. A. Thorley, B. Stolpe, J. Mazzolini, R. J. Dyson and J. Z. Rappoport, Cellular entry of nanoparticles via serum sensitive clathrin-mediated endocytosis, and plasma membrane permeabilization, *International journal of nanomedicine*, 2012, **7**, 2045.
14. K. L. Chen and G. D. Bothun, Nanoparticles meet cell membranes: probing nonspecific interactions using model membranes, *Journal*, 2013.
15. P. Walde, K. Cosentino, H. Engel and P. Stano, Giant Vesicles: Preparations and Applications, *ChemBioChem*, 2010, **11**, 848-865.
16. S. F. Fenz and K. Sengupta, Giant vesicles as cell models, *Integrative Biology*, 2012, **4**, 982-995.
17. A. Czogalla, M. Grzybek, W. Jones and U. Coskun, Validity and applicability of membrane model systems for studying interactions of peripheral membrane proteins with lipids, *Biochimica et Biophysica Acta (BBA)-Molecular and Cell Biology of Lipids*, 2014, **1841**, 1049-1059.
18. E. Sezgin, H.-J. Kaiser, T. Baumgart, P. Schwille, K. Simons and I. Levental, Elucidating membrane structure and protein behavior using giant plasma membrane vesicles, *Nature protocols*, 2012, **7**, 1042.
19. M. Zhang, X. Wei, L. Ding, J. Hu and W. Jiang, Adhesion of CdTe quantum dots on model membranes and internalization into RBL-2H3 cells, *Environ. Pollut.*, 2017, **225**, 419-427.
20. A. Dubavik, E. Sezgin, V. Lesnyak, N. Gaponik, P. Schwille and A. Eychmüller, Penetration of amphiphilic quantum dots through model and cellular plasma membranes, *Acs Nano*, 2012, **6**, 2150-2156.
21. C. Montis, V. Generini, G. Boccalini, P. Bergese, D. Bani and D. Berti, Model lipid bilayers mimic non-specific interactions of gold nanoparticles with macrophage plasma membranes, *J. Colloid Interface Sci.*, 2018, **516**, 284-294.
22. S. Li and N. Malmstadt, Deformation and poration of lipid bilayer membranes by cationic nanoparticles, *Soft Matter*, 2013, **9**, 4969-4976.

23. L. Wang and N. Malmstadt, Interactions between charged nanoparticles and giant vesicles fabricated from inverted-headgroup lipids, *J. Phys. D: Appl. Phys.*, 2017, **50**, 415402.
24. E. Rascol, J.-M. Devoisselle and J. Chopineau, The relevance of membrane models to understand nanoparticles–cell membrane interactions, *Nanoscale*, 2016, **8**, 4780-4798.
25. C. S. Hughes, S. Foehr, D. A. Garfield, E. E. Furlong, L. M. Steinmetz and J. Krijgsveld, Ultrasensitive proteome analysis using paramagnetic bead technology, *Molecular Systems Biology*, 2014, **10**, 757.
26. K. S. Horger, D. J. Estes, R. Capone and M. Mayer, Films of agarose enable rapid formation of giant liposomes in solutions of physiologic ionic strength, *J. Am. Chem. Soc.*, 2009, **131**, 1810-1819.
27. A. Weinberger, F.-C. Tsai, Gijsje H. Koenderink, Thais F. Schmidt, R. Itri, W. Meier, T. Schmatko, A. Schröder and C. Marques, Gel-Assisted Formation of Giant Unilamellar Vesicles, *Biophys. J.*, 2013, **105**, 154-164.
28. Rafael B. Lira, R. Dimova and Karin A. Riske, Giant Unilamellar Vesicles Formed by Hybrid Films of Agarose and Lipids Display Altered Mechanical Properties, *Biophys. J.*, 2014, **107**, 1609-1619.
29. J. S. Hansen, J. R. Thompson, C. Hélix-Nielsen and N. Malmstadt, Lipid Directed Intrinsic Membrane Protein Segregation, *J. Am. Chem. Soc.*, 2013, **135**, 17294-17297.
30. M. G. Gutierrez and N. Malmstadt, Human Serotonin Receptor 5-HT1A Preferentially Segregates to the Liquid Disordered Phase in Synthetic Lipid Bilayers, *J. Am. Chem. Soc.*, 2014, **136**, 13530-13533.
31. A. Gessner, A. Lieske, B. R. Paulke and R. H. Müller, Functional groups on polystyrene model nanoparticles: influence on protein adsorption, *Journal of Biomedical Materials Research Part A: An Official Journal of The Society for Biomaterials, The Japanese Society for Biomaterials, and The Australian Society for Biomaterials and the Korean Society for Biomaterials*, 2003, **65**, 319-326.
32. M. Hadjidemetriou, Z. Al-Ahmady, M. Mazza, R. F. Collins, K. Dawson and K. Kostarelos, In vivo biomolecule corona around blood-circulating, clinically used and antibody-targeted lipid bilayer nanoscale vesicles, *ACS nano*, 2015, **9**, 8142-8156.
33. M. Lundqvist, J. Stigler, G. Elia, I. Lynch, T. Cedervall and K. A. Dawson, Nanoparticle size and surface properties determine the protein corona with possible implications for biological impacts, *Proceedings of the National Academy of Sciences*, 2008, **105**, 14265-14270.
34. T. Cedervall, I. Lynch, M. Foy, T. Berggård, S. C. Donnelly, G. Cagney, S. Linse and K. A. Dawson, Detailed identification of plasma proteins adsorbed on copolymer nanoparticles, *Angew. Chem. Int. Ed.*, 2007, **46**, 5754-5756.
35. A. Verma and F. Stellacci, Effect of Surface Properties on Nanoparticle–Cell Interactions, *Small*, 2010, **6**, 12-21.
36. H. Zhang, X. Wei, L. Liu, Q. Zhang and W. Jiang, The role of positively charged sites in the interaction between model cell membranes and γ-Fe2O3 NPs, *Sci. Total Environ.*, 2019, **673**, 414-423.
37. B. Wang, L. Zhang, S. C. Bae and S. Granick, Nanoparticle-induced surface reconstruction of phospholipid membranes, *Proceedings of the National Academy of Sciences*, 2008, **105**, 18171.
38. S. M. Hussain, K. L. Hess, J. M. Gearhart, K. T. Geiss and J. J. Schlager, In vitro toxicity of nanoparticles in BRL 3A rat liver cells, *Toxicology in Vitro*, 2005, **19**, 975-983.
39. A. Kroll, M. H. Pillukat, D. Hahn and J. Schnekenburger, Interference of engineered nanoparticles with in vitro toxicity assays, *Arch. Toxicol.*, 2012, **86**, 1123-1136.
40. V. Mirshafiee, R. Kim, M. Mahmoudi and M. L. Kraft, The importance of selecting a proper biological milieu for protein corona analysis in vitro: Human plasma versus human serum, *The International Journal of Biochemistry & Cell Biology*, 2016, **75**, 188-195.
41. V. Forest, M. Cottier and J. Pourchez, Electrostatic interactions favor the binding of positive nanoparticles on cells: A reductive theory, *Nano Today*, 2015, **10**, 677-680.
42. H. Keller, M. Lorizate and P. Schwille, PI (4, 5) P2 degradation promotes the formation of cytoskeleton - free model membrane systems, *Chemphyschem*, 2009, **10**, 2805-2812.
43. S. Nazemidashtarjandi and A. M. Farnoud, Membrane outer leaflet is the primary regulator of membrane damage induced by silica nanoparticles in vesicles and erythrocytes, *Environmental Science: Nano*, 2019, **6**, 1219-1232.
44. S. Maktabi, J. W. Schertzer and P. R. Chiarot, Dewetting-induced formation and mechanical properties of synthetic bacterial outer membrane models (GUVs) with controlled inner-leaflet lipid composition, *Soft matter*, 2019, **15**, 3938-3948.
45. H. I. Alkhammash, N. Li, R. Berthier and M. R. de Planque, Native silica nanoparticles are powerful membrane disruptors, *PCCP*, 2015, **17**, 15547-15560.

46. J. C. Bischof, J. Padanilam, W. H. Holmes, R. M. Ezzell, R. Lee, R. G. Tompkins, M. L. Yarmush and M. Toner, Dynamics of cell membrane permeability changes at supraphysiological temperatures, *Biophys. J.*, 1995, **68**, 2608-2614.
47. E. Baykal-Caglar, E. Hassan-Zadeh, B. Saremi and J. Huang, Preparation of giant unilamellar vesicles from damp lipid film for better lipid compositional uniformity, *Biochimica et Biophysica Acta (BBA)-Biomembranes*, 2012, **1818**, 2598-2604.
48. E. M. Gray, G. Díaz-Vázquez and S. L. Veatch, Growth conditions and cell cycle phase modulate phase transition temperatures in RBL-2H3 derived plasma membrane vesicles, *PloS one*, 2015, **10**, e0137741.
49. R. Kuboi, T. Shimanouchi, M. Yoshimoto and H. Umakoshi, Detection of protein conformation under stress conditions using liposomes as sensor materials, *Sensors and Materials*, 2004, **16**, 241-254.
50. R. Koynova and R. C. MacDonald, Natural lipid extracts and biomembrane-mimicking lipid compositions are disposed to form nonlamellar phases, and they release DNA from lipoplexes most efficiently, *Biochimica et Biophysica Acta (BBA)-Biomembranes*, 2007, **1768**, 2373-2382.
51. R. Macháň and M. Hof, Lipid diffusion in planar membranes investigated by fluorescence correlation spectroscopy, *Biochimica et Biophysica Acta (BBA) - Biomembranes*, 2010, **1798**, 1377-1391.
52. S. Sankhagowit, S.-H. Wu, R. Biswas, C. T. Riche, M. L. Povinelli and N. Malmstadt, The dynamics of giant unilamellar vesicle oxidation probed by morphological transitions, *Biochimica et Biophysica Acta (BBA) - Biomembranes*, 2014, **1838**, 2615-2624.
53. K. A. Runas and N. Malmstadt, Low levels of lipid oxidation radically increase the passive permeability of lipid bilayers, *Soft Matter*, 2015, **11**, 499-505.
54. Z. Xia, A. Woods, A. Quirk, I. J. Burgess and B. L. T. Lau, Interactions between polystyrene nanoparticles and supported lipid bilayers: impact of charge and hydrophobicity modification by specific anions, *Environmental Science: Nano*, 2019, **6**, 1829-1837.
55. K. Jacobson, Lateral diffusion in membranes, *Cell motility*, 1983, **3**, 367-373.
56. M. Przybylo, J. Sýkora, J. Humpolíčková, A. Benda, A. Zan and M. Hof, Lipid diffusion in giant unilamellar vesicles is more than 2 times faster than in supported phospholipid bilayers under identical conditions, *Langmuir*, 2006, **22**, 9096-9099.
57. A. M. Farnoud and S. Nazemidashtarjandi, Emerging investigator series: interactions of engineered nanomaterials with the cell plasma membrane; what have we learned from membrane models?, *Environmental Science: Nano*, 2019, **6**, 13-40.

Table of Contents Entry for:

Effect of protein corona on nanoparticle-plasma membrane and nanoparticle-biomimetic membrane interactions

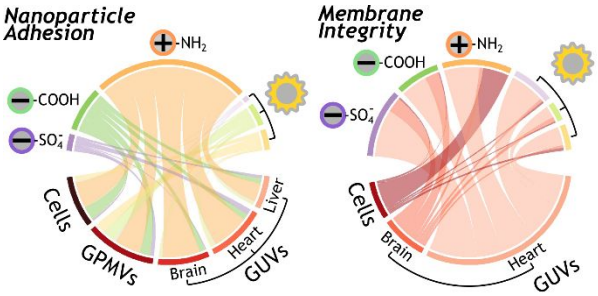

A systematic study of the protein corona's effect on nanoparticle-biomembrane electrostatic interactions. Nanoparticle adhesion and membrane integrity upon nanoparticle-biomembrane interaction were compared between plasma membranes and biomimetic membranes.